Electric current-driven spectral tunability of surface plasmon polaritons in gold coated tapered fibers

Cite as: AIP Advances **8**, 095113 (2018); https://doi.org/10.1063/1.5046991
Submitted: 04 July 2018 . Accepted: 11 September 2018 . Published Online: 20 September 2018

Tilman Lühder, Torsten Wieduwilt, Henrik Schneidewind, and Markus A. Schmidt

Electric current-driven spectral tunability of surface plasmon polaritons in gold coated tapered fibers

Tilman Lühder,[1] Torsten Wieduwilt,[1] Henrik Schneidewind,[1]
and Markus A. Schmidt[1,2,a]
[1]*Leibniz Institute for Photonic Technologies, Albert-Einstein-Str. 9, 07745 Jena, Germany*
[2]*Otto Schott Institute of Material Research, Fraunhoferstr. 6, 07743 Jena, Germany*

(Received 4 July 2018; accepted 11 September 2018; published online 20 September 2018)

Here we introduce the concept of electrically tuning surface plasmon polaritons using current-driven heat dissipation, allowing controlling plasmonic properties via a straightforward-to-access quantity. The key idea is based on an electrical current flowing through the plasmonic layer, changing plasmon dispersion and phase-matching condition via a temperature-imposed modification of the refractive index of one of the dielectric media involved. This scheme was experimentally demonstrated on the example of an electrically connected plasmonic fiber taper that has sensitivities >50000 nm/RIU. By applying a current, dissipative heat generated inside metal film heats the surrounding liquid, reducing its refractive index correspondingly and thus modifying the phase-matching condition to the fundamental taper mode. We observed spectral shifts of the plasmonic resonance up to 300 nm towards shorter wavelength by an electrical power of ≤ 80 mW, clearly showing that our concept is important for applications that demand precise real-time and external control on plasmonic dispersion and resonance wavelengths. https://doi.org/10.1063/1.5046991

INTRODUCTION

Due to unique properties such as nanoscale light confinement and customized dispersion, surface plasmon polaritons (SPPs) have attracted substantial attention by the photonics community during recent times with applications in areas such as bioanalytics,[1] nonlinear photonics[2] and quantum technology.[3] The strong field concentration to metal/dielectric interfaces imposes SPP dispersions to be highly susceptible to the present refractive index (RI) environment, which is utilized in various applications particular within the domain of sensing (e.g., molecular sensing[4] and disease diagnostics[5]). For instance, DNA-based molecular binding processes change the RI at the nanoscale level within the domain of the evanescent field of the SPP, which leads to a modification of the plasmonic dispersion.[6]

To macroscopically detect a change of the plasmonic dispersion, the SPP mode is often phase-matched to a second mode whose properties can be detected by spectroscopic measurements. Therefore the effect of a changing RI environment is transferred from microscopic scales to a measureable signal via a mode coupling scheme. Beside prism coupling,[7] one common technique to spectroscopically detect SPPs is to place the metal/dielectric interface in close proximity of a dielectric waveguide (WG) mode. The two modes involved hybridize,[8] leading to two Eigenmodes that anti-cross close to the wavelength at which the isolated mode dispersions phase-match. Here, energy is exchanged between the two modes, leading to strong dips in the transmission spectrum of the dielectric WG mode that solely arise due to the presence of the SPP.[9] This type of SPP-detection scheme is widely used and is implemented using either planar WGs or[10] plasmonic optical fiber tapers.[11]

[a]markus-alexander.schmidt@uni-jena.de

Particular the latter is highly attractive from the applications point of view since it provides a platform that is compatible with fiber circuitry and which can be integrated into microfluidics. Beside using localized plasmon modes,[12] various types of metal coated tapers (gold,[6] silver[13] and Niobium[14]) have been implemented, revealing a great potential for bioanalytical applications, particular since very high RI sensitivities (>1μm/RIU) have been experimentally demonstrated.

For all mentioned experiments, the phase-matching (PM) wavelength ought to be located in a specific spectral domain to account for the addressed application, which is sometimes hard to achieve due to fabrication inaccuracies or inadequate knowledge on RI. Moreover, application sometimes demand to change the PM wavelength in real-time in order to adapt to the specific experimental prerequisite. These two issues clearly highlight the need for a scheme that allows changing the RI environment in almost real-time in a controlled manner, ideally using a straightforward-to-address external quantity.

Here, we introduce the concept of electrically tuning surface plasmon polaritons using heat dissipation. The key principle is to externally change the dispersion of a propagating plasmon mode via a temperature-imposed modification of the RI of one of the dielectric media involved, with the temperature modification induced by an electric current that flows through the plasmonic layer. This scheme was experimentally demonstrated here on the example of a plasmonic fiber taper with a SPP resonance in the VIS or NIR domains, showing sensitivities of more than 50 000 nm/RIU. We observed spectral shifts of more than 300 nm by electrical powers of about 80 mW that solely arise due to the presence of a dielectric with strong thermo-optical response.

CONCEPT

The overall idea of the tuning concept discussed here is to generate electrical current-driven dissipative heat inside the plasmonic layer that heats up the dielectric surrounding the metal film. This increased temperature imposes the RI of the dielectric to change, which, in turn, modifies the PM conditions between dielectric and plasmonic mode, leading to a macroscopically measurable spectral shift of the SPP resonance.

The impact of a changing temperature on the PM wavelength can be qualitative understood by the following toy-model that is related to an SPP located at a planar gold/dielectric interface (dielectric function of gold can be found in Ref. 15, top sketch in Fig. 2): In case both materials show a thermo-optical response, the effective index of this single interface SPP can be written as:

$$n_{eff} = \sqrt{\left(\varepsilon_m(\sigma_m, \lambda, T) \cdot n_d^2(\sigma_d, \lambda, T)\right) / \left(\varepsilon_m(\sigma_m, \lambda, T) + n_d^2(\sigma_d, \lambda, T)\right)} \quad (1)$$

with the dielectric susceptibility of the metal $\varepsilon_m(\lambda, T)$ and the RI of the dielectric $n_d(\sigma, T, \lambda)$, with the metal and dielectric thermo-optic coefficients σ_m and σ_d, the temperature T and the wavelength λ. Assuming a directional mode coupling situation that provides PM to occur at the room temperature T_0 and the wavelength λ_0, the corresponding effective index at the PM point is given by $n_{PM} = n_{eff}(\sigma_m, \sigma_d, T_0, \lambda_0)$. In a first order approximation, the dispersion of n_{PM} can be neglected, allowing to analyse the behaviour of the PM wavelength λ_{PM} as function of T and thermo-optic coefficients via the equation $n_{PM} = n_{eff}(\sigma_m, \sigma_d, T, \lambda_{PM})$. Assuming a negative thermo-optic coefficient, which is characteristic for many liquid materials,[16] and a room temperature RI of the dielectric of $n_d(T_0, \lambda_0) = 1.45$, a strong decrease of λ_{PM} for an increasing temperature is found (Fig. 2, thermo-optic coefficient of gold at 830 nm: $4.9 \cdot 10^{-4}$ K^{-1} [17]). Although the magnitude of the thermo-optic coefficient of gold is comparable to that of liquids and included in the model, its impact on the PM wavelength shift is negligible (>0.31 nm for all situations presented here). Particular in case the liquid thermo-optic coefficient σ_d is smaller than $-1 \cdot 10^{-4}$ K^{-1}, spectral shift of the order of tens of nanometres can easily be achieved within an temperature interval less than 50 K, revealing that a strong spectral shift can be realized within a straightforwardly accessible temperature domain.

Within the scope of this work the temperature inside the dielectric was changed by means of dissipative heat generated inside a plasmonic film that is electrically connected to a power supply. Moving electrons, accelerated by the applied voltage V, collide with metal ions and are scattered in arbitrary directions. Randomly moving charges constitute thermal motion and dissipative heat is created across the entire circuitry with its power proportionally to the local resistance R

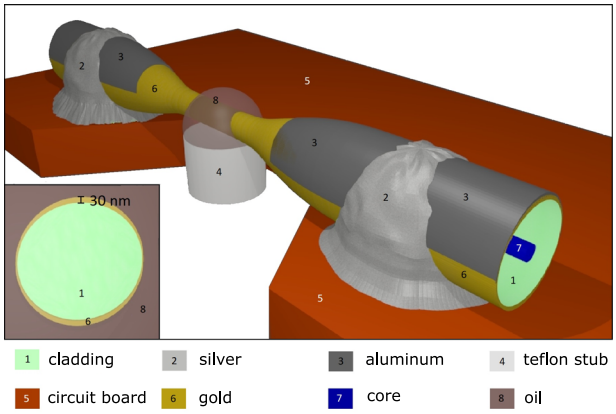

FIG. 1. Sketch of the experimentally used device to demonstrate the concept of electrically tuning surface plasmon polaritons via current-driven heat dissipation. The structure consists of a plasmonic fiber taper that is electrically connected and partially surrounded by a liquid that exhibits a strong thermo-optical response, promoting phase-matching between plasmonic and photonic modes. The inset shows a cross section of the taper inside the waist region (23 µm width, both not to scale, colour online).

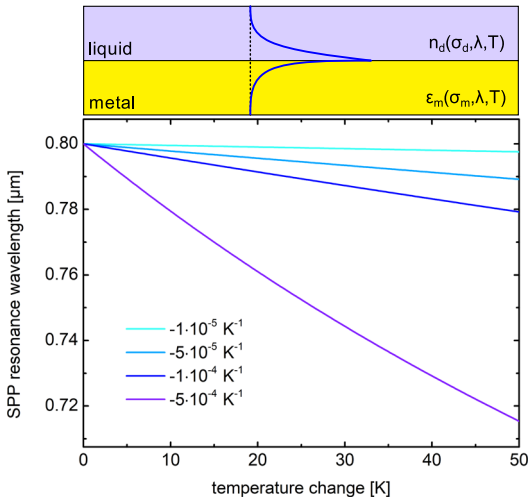

FIG. 2. Toy model (top sketch, the blue curve shows the dominant magnetic field component) that allows to qualitatively understand the impact of a changing temperature on the phase-matching wavelength of a planar SPP propagating on a gold/dielectric interface ($\lambda_0 = 800$ nm, $n_{PM} = 1.45$). The different curves in the main plot refer to various thermo-optical coefficients of the dielectric (defined in the legend from top to bottom, colour online).

(Joule heating $P = I^2 \cdot R$,[18] electric current I). For the geometry considered here the highest resistance per length L is found in the taper waist. Calculations based on a cosine shaped cross-section area A of the metal, measured taper diameters and Pouillet's law $R/L = \rho A$ (ρ is the resistivity, $\rho_{Au} = 2.2$ µΩcm,[19] $\rho_{Al} = 2.61$ µΩcm[20]) indicate that 79 % of the electrical power is transformed into dissipative heat within the pure gold coated waist section. 28 % of the total heat is created within the region of the SPP propagation (oil region, Fig. 1) and is transferred to the dielectric via conduction, neglecting the remaining circuit outside the taper contact points.

SAMPLE STRUCTURE AND SAMPLE FABRICATION

The structure that has been created to demonstrate the concept of electrically tuning SPPs using heat dissipation is a metal coated fiber optical taper (Fig. 1). As explained more in detail in ref 21, 14, the fundamental taper mode couples to the SPP mode supported by the metal film, imposing modal

TABLE I. Comparison of thermo-optic coefficients for all involved materials and maximum refractive index change for 50 K Temperature increase (at a wavelength of 830 nm).

material	Cargille oil n_D = 1.40	Cargille oil n_D = 1.42	Cargille oil n_D = 1.436	gold	fused silica
dn/dT [K^{-1}]	$-4.12 \cdot 10^{-4}$	$-4.04 \cdot 10^{-4}$	$-3.97 \cdot 10^{-4}$	$4.9 \cdot 10^{-4}$	$8.6 \cdot 10^{-6}$ [27]
Δn for ΔT = 50 K	-0.0206	-0.0202	-0.0199	0.0245	0.00043

hybridization[8] and a distinct peak in the transmission spectrum of the fundamental taper mode at the plasmonic/photonic PM wavelength. The respective resonance wavelength λ_R is dependent on the layer thickness, waist diameter and, most importantly, on the RI of the most outer medium which is controlled here by dissipative heat.[22–25] The electrically active plasmonic fiber taper has been implemented by tapering a single mode fiber (780HP, cut-off wavelength 730 nm), using a Vytran GPX 3000 (AMS Technologies AG), which was sputtered and electrically connected to provide a longitudinal flow of electrical current through the metal. The final taper has a waist diameter and length of (23 ± 1) µm and 1 cm, respectively, embedded between two 35 mm long adiabatic transitions to ensure excitation of the fundamental taper mode only. As next step the fiber is coated on two opposite sides with gold by DC magnetron sputtering process (Ar pressure: 0.5 Pa, depositin rate: 0.41 nm/s), leading to two sickle-shaped metallic layers (maximum thickness 30 nm, structure shown in the inset of Fig. 1). Since the gold film thickness is not zero at any position around the circumference of the taper, the two gold stripes are electrically connected. Using preliminary modal simulations, the geometrical parameters were chosen such to obtain spectrally sharp resonance dips in case the taper is immersed in liquids (here oils) with high RI.

Outside the taper waist the electric conductance is enhanced by an additional aluminum layer (thickness (450 ± 30) nm) created by thermal evaporation on one side of the fiber (Fig. 1, the waist was protected by a mask to avoid Al deposition on the plasmonically relevant region). Although the adhesion of gold on silica is rather poor, no intermediate layer was added such not to undesirably change the optical properties of the gold film.[26] To provide electrical connections the fiber is placed onto a circuit board and mechanically fixed by conductive silver. The total resistivity of this arrangement is about 420 Ω, which is low compared to the case no Al is used (1-2 kΩ) and, more importantly, increases the fraction of total heat generated in the liquid section up to five times. As shown in preliminary experiments the contact positions must be at least 1.5 cm away from the ends of the waist regions not to have any influence on the transmission, whereas here we choose a separation distance of 2 cm to be on the safe side.

To provide PM between plasmonic and taper modes, a defined section of the taper waist (length 2.8 mm) was immersed into the mentioned oils which have precisely known material dispersion (Cargille RI oils, identified by the base RI n_D at 589 nm and 25 °C), increasing the RI of the most outer dielectric influencing the SPP dispersion such to provide PM. Due to their large negative thermo-optical coefficient (see Table I, fused silica as reference 27), the RI of the liquid decreases in case the current-driven heat is increased. For instance a temperature increase of 50 K imposes the RI of a particular liquid (n_D = 1.42) to decrease from 1.42 to 1.3998.

OPTICAL SETUP

The optical setup used to determine the spectral properties of the light transmitted through the taper consists of a broadband light source, coupling optics, the sample under investigation and spectral diagnostics. Specifically, polarized light from a supercontinuum source (SuperK Compact, NKT Photonics) was coupled into and out of the fiber via objectives (Edmund optics, 20 x, NA = 0.4) The transmitted signal was guided to an optical spectrum analyzer (Ando AQ6317B) via another step-index fiber (HP-780). The input polarization direction was adjusted such to obtain the largest fringe contrast at the resonance wavelength, which matches the direction of maximum gold thickness, i.e., corresponds to a transverse-magnetic (TM) configuration. Before coupling into the single-mode fiber the output light was filtered by a second polarizer oriented parallel to the input polarizer (both LPVIS050, Thorlabs) to prevent cross polarization effects. A complete sketch of the

setup is shown in Fig. 6 of ref. 14. Wavelengths close to 1064 nm that result from the supercontinuum pump laser have been blocked by a notch filter (NF 1064-44) to suppress residual heating, whereas in situations the resonance is located at wavelength <1 μm a short pass filter (FES1000) was used. The size of the Teflon stub that supports the oils determines the SPP/taper mode interaction length, which in the present case is 2.8 mm. The obtained spectra are normalized to the transmission of the taper without oil, which show no resonance in the spectral domain of interest.

HEAT CONTROLLING SETUP

The electrical current to heat up the fiber is provided by a constant voltage power supply (type 3230.1, Statron Gerätetechnik GmbH). First, the output voltage is double checked using a sensitive Multimeter (model 2010, Keithley Instruments). Second, the taper is electrically connected, where more than half of the total wavelength shift occurs within the first 6 seconds. Then the resonance wavelength decreases exponentially towards the equilibrium value with a time constant of about 40 seconds. The experiments show that 3-5 Minutes are sufficient to wait until the system has reached thermal equilibrium. Since Joule's first law predicts a heating proportional to the applied electrical power as product of electrical current and voltage, we used the electrical power as the reference parameter which is externally modified, i.e., which is analyzed in regard of the spectral shift of the resonance. This is particularly useful, because it includes the increase of resistance of the taper with temperature ($\sim$1.46 $\Omega \cdot K^{-1}$), accumulating to more than 50 Ω within the used temperature range.

Temperature changes in close proximity to the relevant region have been measured by a fiber optical sensor, placed orthogonal to the taper inside the oil above the waist. The actual temperature sensitive element here is a self-made Fabry-Pérot-interferometer consisting of a pair of low RI SiO_2 layers (thickness λ/4) embedded in high RI silicon on the fiber tip. White light is send into the fiber sensor and the back-reflection is analyzed with a spectrometer by tracking the reflection dip minimum. Calibration of this device using a temperature bath reveals a sensitivity of (0.0690 ± 0.0003) $nm \cdot K^{-1}$ enabling us to measure the temperature very precisely down to Kelvin scales in micrometer distance to the taper. No mechanical contact to the waist was made in order not to damage the gold layer. Since the evanescent field of the SPP inside the oil is only a few hundred nanometers, the temperature sensor is not affecting the taper.[28] As only a small part of the spectrum is transmitted out of the sensor any heating originating from the sensor itself was negligible.

RESULTS: TRANSMISSION MEASUREMENTS

The transmission spectra (Fig. 3) show that the SPP-resonance peaks strongly shift towards longer wavelength with an increasing fringe contrast in case the RI of the applied oil is increased. Here, only one main dip is visible in each spectrum, indicating that the two gold sickles have similar geometrical shapes. Particular at long wavelengths additional features appear in the transmission spectra, which result from higher-order azimuthal modes that emerge as a consequence of the azimuthal dependence of the gold film thickness.[23,24,29] Due to their low fringe contrast, however, the subsequent discussion solely focuses on the main dip which is associated with the fundamental plasmon resonance of the double-sickle geometry. Limitations of the fiber guidance combined with high attenuation restrict the measurements to a maximum oil RI of n_D = 1.436.

RESULTS: TAPER SENSITIVITY

In order to get a calibration curve that relates the RI of the oil to λ_R, the absorption peaks are fitted by Gaussian functions and the respective dip wavelengths are plotted against the RI of the oil (inset of Fig. 4). Please note that the x-axis of this plot refers to the RI of the oil at the resonance wavelength, which was calculated by using a Cauchy equation provided by the manufacturer and at room temperature of 20.5 °C (n_D = 1.40, n_D = 1.42 and n_D = 1.436 correspond to n = 1.393, n = 1.4109 and n = 1.4236, respectively). These two corrections (material dispersion and temperature) contribute uncertainties up to 0.004 RIU, which are indicated by error bars in inset of Fig. 4. Not taken into account is the additional heating by the incident light, which depends on the total absorbed

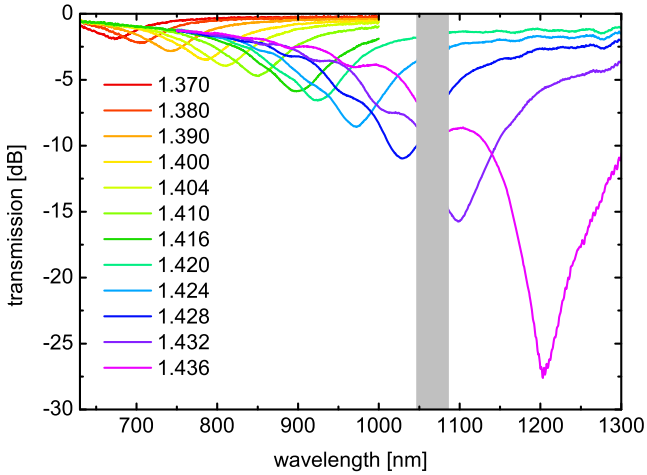

FIG. 3. Spectral distribution of the transmission of the plasmonic fiber taper (details can be found in the main text) in case 2.8 mm of the taper waist is exposed to different RI oils (the different curves refer to the various oils used (numbers are related to the RI of the respective oil at 589 nm and 25 °C for the measured curves from left to right, colour online)). Wavelengths around 1064 nm have been blocked (indicated by the gray bar) by a notch filter to suppress light-induced heating by the supercontinuum source driving laser.

power and, due to Lambert-Beer's law, the longitudinal location of the mode inside the liquid. The temperature difference across the liquid is measured to be 1.5 K for n_D = 1.436 by longitudinally scanning with the fiber temperature sensor along the waist, overall broadening the SPP resonance dip. Furthermore, transmission measurements for different light powers indicate a temperature rise due to light absorption and plasmon decay to be effectively 1.2 K, 3.1 K and 5.0 K for the liquids with n_D = 1.40, n_D = 1.42 and n_D = 1.432, respectively. The additional heating of the gold layer based on different incident light powers due to filter changes for PM wavelength >900 nm was compensated by an temperature offset of 3.7 K, based on matching PM wavelengths of specific RI oils (n_D = 1.424 and 1.420), where both sets of filters could be applied. The combined data in the inset of Fig. 4 suits an error bar weighted fit of a sum of two exponential functions. This ansatz was chosen over a polynomial one to get a smooth curve for both fit and its derivative. The latter is the in the main plot of Fig. 4 presented sensitivity of our taper. The sensitivity increases towards larger RIs to more than

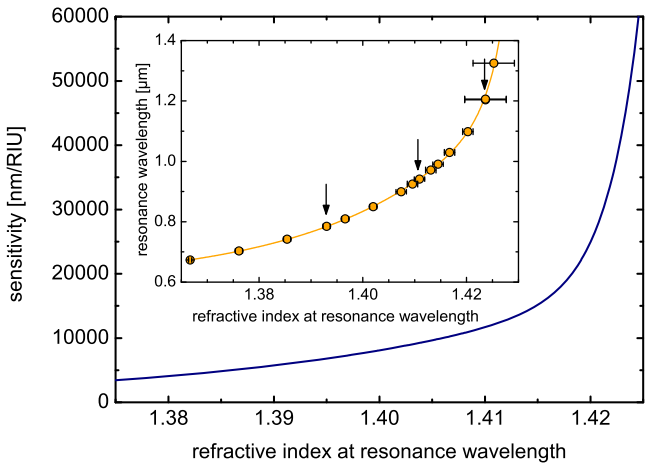

FIG. 4. Refractive index sensitivity of the plasmonic fiber taper vs. refractive index of the used oil at the corresponding resonance wavelength. Inset: Measured resonance wavelengths for different oil refractive indices (at the resonance wavelength). The points are the experimental measured resonance wavelengths, whereas the orange curve is a double exponential fit (see main text) to the data points and was used to calculate the sensitivity shown in the main plot. Arrows indicate the starting resonance wavelengths at $U = 0$ for the three liquids used in electrical experiments below.

50000 nm/RIU at $n = 1.425$, enhanced by the temperature rise due to increased light absorption. This value is comparable to those reported by Monzón-Hernández[23] as well as theoretical predictions[6] and is higher than the ones presented for other plasmonic refractometer designs such as D-shaped fibers or integrated waveguides.[25,30,31]

RESULTS: ELECTRO-ACTIVE CHANGE OF TRANSMISSION PROPERTIES

The next step of the experiments includes the analysis of the current-induced spectral shift of the SPP resonances (Fig. 5). Increasing the current (i.e., applied electric power) imposes the plasmonic resonance to shift to shorter wavelengths (green curve in Fig. 6), which overall is a result of the combination of dissipative heat and negative thermo-optical response. The higher temperature lowers the RI of the oils according to Table I, shifting the SPP resonance peak up to 137 nm towards shorter wavelengths in case of an electric power of 76 mW (n_D = 1.42). The resonance peak wavelength is expected to decrease even further for higher powers which, however, were not tested here to prevent sample damaging. The spectral shift is independent on the sign of the applied voltage (not presented here), verifying that dissipative heating is the origin of the observed effect and that any current-driven thermal contribution imposed by the aluminum/gold interface is either too small to be measured or negligible since the region of interest is in the center of both interfaces, leading to an effect of opposite sign.[32,33] The nonlinearity of the temperature curves is explained by the stronger heat dissipation from liquid to the environment (air) at overall higher temperatures.

The RI at a fixed value of current, i.e. electric power, can be extracted using the reverse calibration curve (Fig. 4) and PM wavelength of the measured SPP dip. In combination with the known thermo-optic coefficient and the PM wavelength of the oil without voltage this allows us to calculate the temperature change $\Delta T = (n(U) - n(U = 0)) \cdot \sigma^{-1}$, that in the present case is up to 37 K (dark blue line in Fig. 6). The PM wavelength of the reference curve ($U = 0$) of the test series, where the voltage was increased stepwise, (brown, most right curve in Fig. 5) varies slightly compared to the previously done measurement for the calibration of PM wavelength to RI (Fig. 3). This wavelength mismatch of several nanometers is caused by minor temperature, coupling and oil region length disparities. In the evaluation of the temperature, only the reference value of the same test series is utilized. Although the experimentally measured temperature T_{exp} using the Fabry-Pérot thermometer is lower than its calculated counterpart T_{calc}, the order of magnitude of the temperature relevant in the experiments is confirmed. It is important to note that the ratio of measured and calculated temperature is roughly constant for all electric powers applied (inset of Fig. 6), which can be explained by the fact that the temperatures at the locations of taper and external sensor are different, since the sensor is positioned

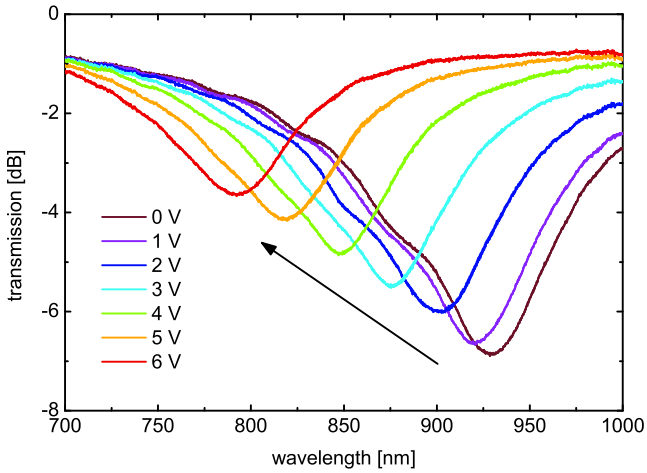

FIG. 5. Spectral distribution of the transmission of the electrically connected plasmonic fiber taper for different applied external voltage (length of liquid along light propagation direction: 2.8 mm, base RI of oil: n_D = 1.420). The black arrow indicates the spectral shift of the resonance towards shorter wavelengths in case the voltage is increased.

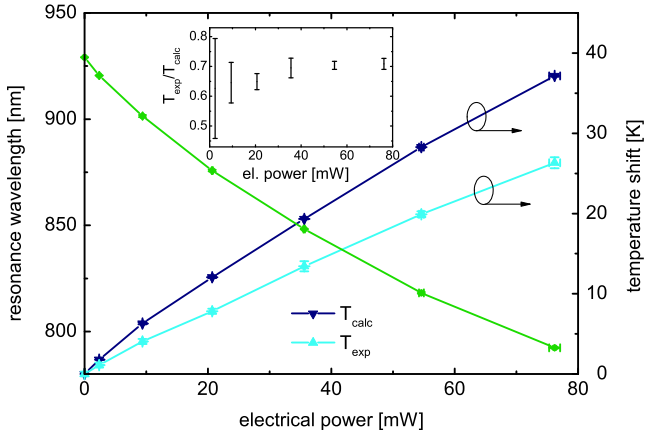

FIG. 6. SPP resonance wavelength of the spectra presented in Fig. 5 (green points, left axis), calculated (dark blue points) and measured (light blue points, both right axis) temperature changes T_{calc} and T_{exp}, respectively, all as functions of applied external electric power. The connecting lines are guides-to-the-eye. The inset shows the ratio of both temperatures at the same electric power.

above the taper. Small drifts of this ratio might occur when the distance of the temperature sensor to the taper varies due to thermal expansion. By increasing the applied current, the overall transmission through the taper increases, reducing the heat generated by light absorption and SPP decay. Compared to the electrical heating the corresponding impact is small (calculated to be ∼-2 K within the full current range for n_D = 1.42) and has the opposite sign. Nevertheless, it could also explain a slight rise of the ratio of calculated to measured temperature. The inaccuracy of the PM wavelength is mainly due to thermal fluctuations resulting in variations of <1 nm for all RI and electrical powers except for n_D = 1.436 at >25 mW, where it increases to 2 nm.

These current-sensitive measurements were repeated for two additional RI oils (n_D = 1.40 (red triangles facing down in Fig. 7) and n_D = 1.436 (blue triangles facing up in Fig. 7)), showing spectral shifts from 776.2 nm to 704.6 nm and 1206.8 nm to 903.4 nm, respectively. The relative wavelength shifts for similar electric powers increase towards larger values of oil RI (inset in Fig. 7). Values as high as 25 % for n_D = 1.436 result from the higher thermo-optic response at longer wavelengths combined with the increased light absorption at similar electric powers.

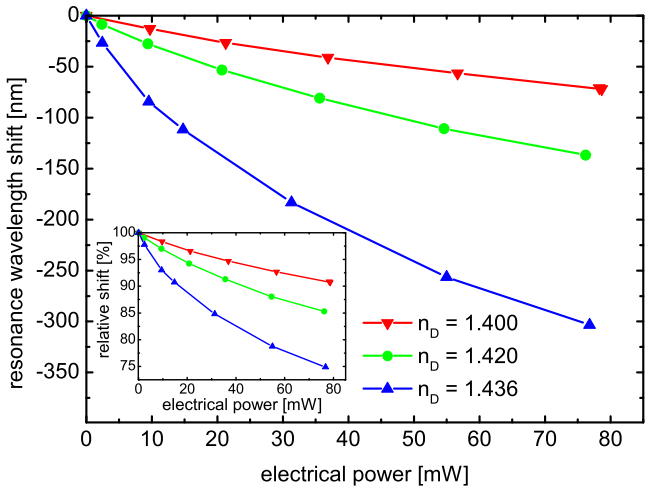

FIG. 7. Dependence of the relative SPP resonance wavelength ($\lambda_R(P) - \lambda_R(P=0)$) on applied electric power for three different RI oils (n_D = 1.4 (red), 1.42 (green) and 1.436 (blue)). The inset shows the identical evolution with the resonance wavelength normalized to the values at zero electric power ($\lambda_R(P)/\lambda_R(P=0)$).

CONCLUSION

Due to their unique properties surface plasmon polaritons found widespread use in various fields of science and application, whereas precise control on dispersion is in many situations challenging, demanding schemes to post-tune the plasmonic optical properties. Here we introduce the concept of electrically tuning surface plasmon polaritons using current-driven heat dissipation into the dielectric layer, allowing controlling plasmonic properties via a straightforward-to-access quantity. The key idea is based on an externally controlled current flowing through the plasmonic layer and changing the dispersion of a propagating plasmon mode via a temperature-imposed modification of the refractive index of one of the dielectric media involved. This scheme, qualitatively shown by a toy model, was experimentally demonstrated on the example of a plasmonic fiber taper embedded in a liquid with strong thermo-optical response, showing plasmonic resonance in the VIS or NIR with sensitivities >50000 nm/RIU. By increasing the temperature inside the liquid via electrically generated dissipative heat, we observed spectral shifts of the plasmonic resonance of up to 300 nm towards shorter wavelength by electrical powers in the range of 80 mW, corresponding to a maximum temperature change of about 40 K. This behavior has been found for various liquids and solely arises due to presence of a dielectric medium with strong thermo-optical response.

Our concept of tuning the spectral response of plasmonic devices via current-driven heat dissipation is highly relevant particular from the application perspective, since the plasmonic resonance can be tuned over hundreds of nanometers just by using a simple electric current supply without changing the actual geometry of the device. Therefore a fluctuating environmental temperature can be compensated for in almost real-time, and, more importantly, the plasmonic resonance can be shifted to a desired spectral domain having implications for fields such as bioanalytics and sensing. Future work will aim to further reduce the liquid volume to improve the device's response time and transfer the concept to planar waveguide technology.

ACKNOWLEDGMENTS

The authors highly acknowledge support from the German Science Foundation (IRTG 2101, SCHM2655/9-1). We acknowledge financial support for publication from Thüringer Universitäts-und Landesbibliothek Jena (ThULB) and Friedrich-Schiller-University (FSU).

[1] S. Sugimoto *et al.*, Commun. Biol. **1**, 52 (2018).
[2] T. Y. F. Tsang, Opt. Lett. **21**, 245 (1996).
[3] J. Tanget *et al.*, Nat. Commun. **9**, 1705 (2018).
[4] R. Karlsson and R. Stahlberg, Anal. Biochem. **228**, 274 (1995).
[5] K. Hegnerová *et al.*, Sens. Actuators, B **139**, 69 (2009).
[6] T. Wieduwilt *et al.*, Plasmonics **8**, 545 (2013).
[7] E. Kretschmann *et al.*, Z. Naturforsch., A: Phys. Sci. **23**, 2135 (1968).
[8] A. Tuniz and M. A. Schmidt, Opt. Express **24**, 7507 (2016).
[9] H. W. Lee *et al.*, Opt. Express **19**, 12180 (2011).
[10] J. Dostálek *et al.*, Sens. Actuators, B **76**, 8 (2001).
[11] A. Diez *et al.*, Electron. Lett. **32**, 1390 (1996).
[12] T. Wieduwilt, APL Photonics **1**, 6 (2016).
[13] N. A. Janunts *et al.*, Opt. Commun. **253**, 118 (2005).
[14] T. Wieduwilt *et al.*, Sci. Rep. **5**, 17060 (2015).
[15] K. M. McPeak *et al.*, ACS Photonics **2**, 326 (2015).
[16] S. Pumpe *et al.*, Opt. Express **25**, 22932 (2017).
[17] C. S. Moreira *et al.*, Sens. Actuators, B **134**, 845 (2008).
[18] H. Lass, *'Vector and Tensor Analysis'* (McGraw-Hill, New York, 1950).
[19] H.-G. Kadereit, Thin Solid Films **1**, 109 (1967).
[20] British Aluminum Co. Ltd, Data sheet.
[21] J.-H. Zhan and S.-M. Tseng, Jpn. J. Appl. Phys., Part 2 **36**, L1390 (1997).
[22] X. Zhou *et al.*, Opt. Commun. **382**, 610 (2017).
[23] D. Monzón-Hernández *et al.*, Appl. Opt. **43**, 1216 (2004).
[24] A. Díez *et al.*, J. Opt. Soc. Am. A **16**, 2978 (1999).
[25] M.-C. Navarrete *et al.*, Sens. Actuators, B **190**, 881 (2014).
[26] T. Siegfried *et al.*, ACS Nano **7**, 2751 (2013).
[27] D. B. Leviton and B. J. Frey, Proc. SPIE **6273**, 62732K (2006).
[28] W. L. Barnes, J. Opt. A: Pure Appl. Opt. **8**, 87 (2006)

[29] A. Diez *et al.*, IEEE Photonics Technol. Lett. **10**, 833 (1998).
[30] R. Slavík *et al.*, Sens. Actuators, B **74**, 106 (2001).
[31] L. A. Obando and K. S. Booksh, Anal. Chem. **71**, 5116 (1999).
[32] R. A. Innes and J. R. Sambles, Solid State Commun. **56**, 493 (1985).
[33] J.-C. Weeber *et al.*, Appl. Phys. Lett. **99**, 031113 (2011).